ISSN 1062-8738, Bulletin of the Russian Academy of Sciences: Physics, 2016, Vol. 80, No. 12, pp. 1489–1493. © Allerton Press, Inc., 2016.
Original Russian Text © V.E. Rogalin, O.M. Kugaenko, E.E. Ashkinazi, M.S. Andreeva, S.A. Filin, 2016, published in Izvestiya Rossiiskoi Akademii Nauk, Seriya Fizicheskaya, 2016, Vol. 80, No. 12, pp. 1688–1692.

Examining Surfaces of Oxidized Aluminum Exposed to CO_2 Laser Pulses

V. E. Rogalin[a, b, *], O. M. Kugaenko[c, **], E. E. Ashkinazi[d, e, *], M. S. Andreeva[f], and S. A. Filin[g]**

[a] *Astrofizika National Center of Laser Systems and Complexes, Moscow, 125424 Russia*
[b] *Tver' State University, Tver', 170100 Russia*
[c] *National University of Science and Technology (MISiS), Moscow, 119049 Russia*
[d] *Prokhorov General Physics Institute, Russian Academy of Sciences, Moscow, 119991 Russia*
[e] *National Research Nuclear University, Moscow Engineering Physics Institute (MEPhI), Moscow, 115409 Russia*
[f] *Moscow State University, Moscow, 119991 Russia*
[g] *Plekhanov Russian University of Economics, Moscow, 117997 Russia*
**e-mail: v-rogalin@mail.ru*
***e-mail: crystal@misis.ru*
****e-mail: ashkinazi@nsc.gpi.ru*

Abstract—Comprehensive microstructure studies of the surfaces of duralumin sheets exposed to an intense microsecond CO_2 laser pulse (E ~ 500 J) are performed for the first time. The irradiated area is ~100 cm^2. A pulse with a duration of ~5 μs has an ~200 ns leading peak. Passivated duralumin sheets subjected to pressure and thermal treatment resulting in the formation of Al_2O_3 layers ~7 μm thick are irradiated. Electron and atomic force microscopy, X-ray spectral analysis, and optical profilometry are used in the study. Detected traces of nonequilibrium evaporation contained a polycrystalline aggregate of several stoichiometric and nonstoichiometric phases of aluminum oxide and its compounds with manganese and magnesium.

DOI: 10.3103/S1062873816120170

INTRODUCTION

Passivation coatings based on Al_2O_3 are often used in aeronautics, mechanical engineering, automotive engineering, special purpose machinery, microelectronics, and other branches of current technology to protect assemblies and parts made from aluminum and its alloys against corrosion in air [1, 2].

The reason for this is the considerable electronegative potential of aluminum. The oxide film that forms as a result of several manufacturing operations does not guarantee 100% protection against corrosion, since such films are highly porous. Dense protective films are commonly produced via anodic oxidation [2]. It is well known that the working surfaces of machine components with such coatings are fairly resistant to corrosive media and heavy erosion and abrasive wear.

Data on the resistance of such coatings to a variety of adverse factors (especially intense laser radiation) are therefore of considerable interest.

The impact of an intense microsecond CO_2 laser pulse on surfaces of metals and other structural materials has been thoroughly studied [3–6]. Low-threshold optical air breakdown starts at a radiation power density of $\geq 10^7$ W cm^{-2} and ambient atmospheric pressure. The resulting plasma absorbs most of the radiation and shields the metal form further exposure to radiation [3–8]. No visible evidence of damage is in this case normally observed on a sample's surface.

The aim of this work was to investigate the effect a single electric-discharge CO_2 laser pulse (E ~ 500 J) [9] has on a surface of oxidized duralumin. The pulse had an ~200 ns leading peak and an ~5 μs tail (Fig. 1). The irradiated area was ~100 cm^2.

The pulse shape was recorded by a photodetector, based on the photon drag effect of holes in germanium, and its energy was measured by a TPI 2-5 ther-

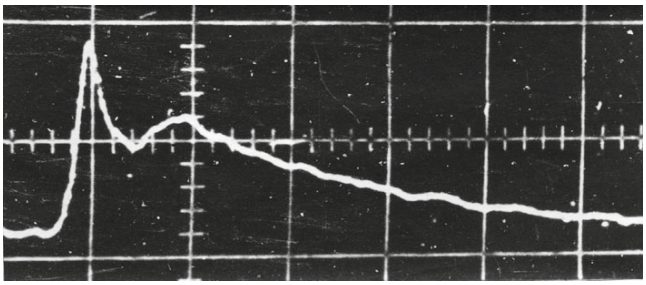

Fig. 1. Shape of a typical laser pulse (0.5 μs/div.) [5, 6, 9, 10].

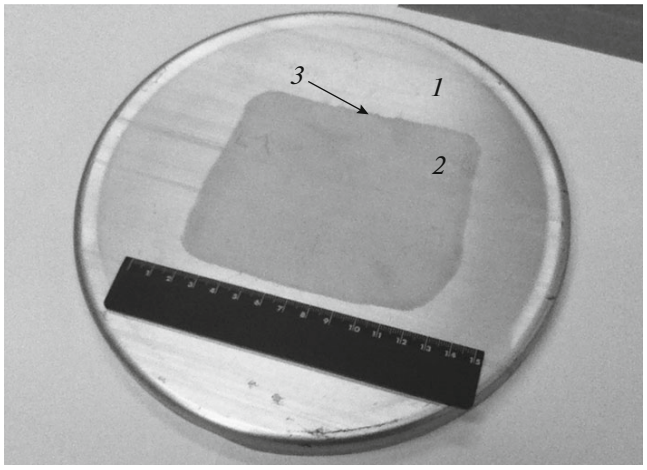

Fig. 2. General view of an irradiated region: (*1*) D16 duralumin disk (d = 200 mm, h = 1 mm); (*2*) mark left by a directed laser pulse; and (*3*) nontransparent boundary of the irradiated region.

mocouple calorimeter. The measuring procedure was described in [4–6, 8–10]. It has been noted in a number of experimental studies of interaction between the radiation of the indicated laser and different materials that only the peak part of a pulse (~20% of the pulse energy; in this case, ~1 J cm^{-2} [4–6, 11]) reaches the sample surface at such radiation energy densities. The so-called complete radiation cutoff is observed approximately 1 μs after the start of generation under these conditions. The tail part is absorbed in the air breakdown plasma, which has a lifetime of ~20–25 μs.

MATERIALS AND METHODS

Plane-parallel disks fabricated by hot pressing from D16 rolled stock were irradiated. These disks had diameters of 20–30 cm and were ~0.1 cm thick. They were oxidized during passivation in air. Laser pulses left characteristic traces on their surfaces that had the same geometric size as the mark left by a laser beam on thermal paper (Fig. 2).

In the area of a trace, a sheet surface assumed a flat white color that did not hide the scratches left after mechanical processing. However, a trace became nontransparent in the ~5–8-mm-wide boundary zone of a spot. Comprehensive microstructure studies were conducted to assess the nature of laser impact and the properties of the material in the irradiated region. Electron and atomic force microscopy, X-ray spectral and structure analysis, and optical profilometry were used in these studies. The surface relief was examined with a Zygo NewView 5000 optical profilometer.

The microstructure was studied at the shared resource center of the National University of Science and Technology (MISiS) using an AXIO Imager D1m optical microscope, a JSM-6480LV (JEOL, Japan) high-resolution electron microscope, and a SNE4500M scanning electron microscope provided by OPTEC.

The phase composition of samples was studied via X-ray diffraction using a Bruker D8 ADVANCE diffractometer with symmetric θ-2θ scans and monochromatized CuK_α radiation (λ = 1.54178 Å) at room temperature. The sample was mounted horizontally and rotated at a rate of 15 rpm. Measurements were performed in the 2θ interval from 20° to 80° with a pitch of 0.1° and 3-s-long exposures at each point. The angular resolution was 0.05°. The results from these measurements were processed using the DIFFRAC software package. Diffraction reflections were identified by matching the experimental interplanar distances to the reference values for a variety of materials (taken from the PDF-2 (2006) database) in EVA.

The elemental compositions of duralumin areas with surfaces passivated in air and areas exposed to laser radiation were examined using a JSM-6480LV (JEOL, Japan) scanning electron microscope with an INCA (Oxford, UK) energy dispersive spectrometry attachment. This attachment allowed us to determine the elemental composition in a volume of approximately 1–3 μm^3 by detecting the characteristic X-ray radiation produced as a result of interaction between the primary electron beam and a sample's surface. The sensitivity of this method was ~0.1 at %, the control voltage was 20 kV, and the probe size varied from 2 to 50000 μm^2.

RESULTS AND DISCUSSION

It was found that the irradiated region of each surface was covered with a dull layer. Marked traces of nonequilibrium evaporation were observed, and each surface was spotted with small craters with characteristic sizes of ~0.1–5 μm (Fig. 3). After laser irradiation, rolling marks (chains of parallel scratches on the metal's surface that were easily seen through the Al_2O_3 layer) were partially discernible. It was also clear that the new defects, which were of a patchy nature, were localized primarily above the rolling defects. Some of them had distinct coloring that differed from the background coloring: white, black, and (at times) red patches were observed. In some regions, well-defined marks left by chipped-out coating grains with a sizes of up to 20 μm were observed (Fig. 3a).

Three- and two-dimensional relief images and cross-section profiles of the initial and irradiated surfaces were obtained using a Zygo NewView 5000 optical profilometer with vertical resolution as high as 0.1 nm. Since an automated positioning stage was available and the images obtained in a single scan could be stitched together using specialized software, it was possible to study surface regions with lateral sizes much larger than the objective's field of view.

Initial examination of the samples revealed two distinct packets of interference lines of radiation

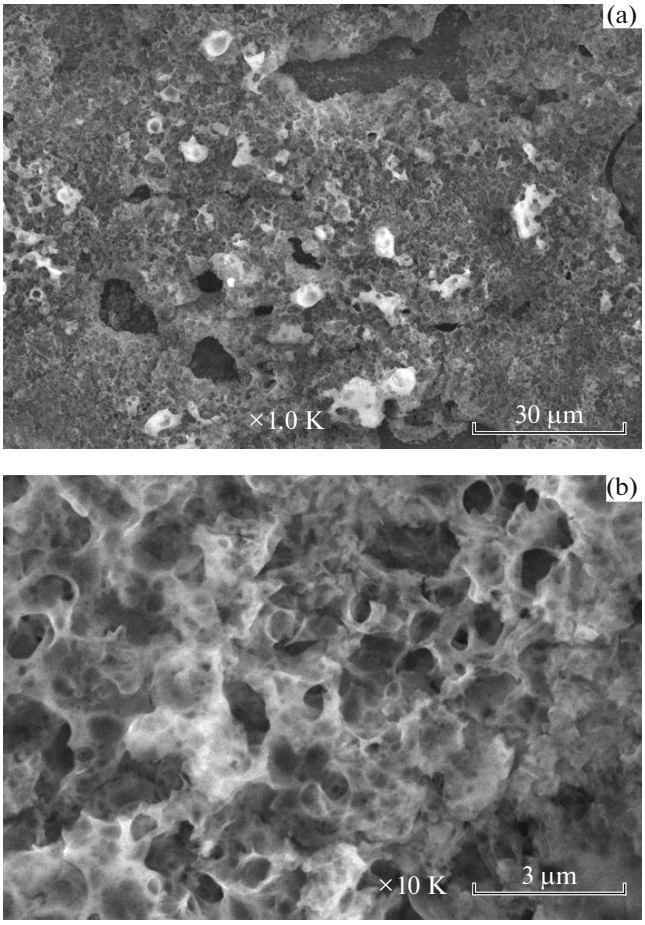

Fig. 3. Images of the oxide film (Al_2O_3) on an Al disk's surface after laser irradiation (a SNE4500M scanning electron microscope provided by OPTEC was used to obtain these images).

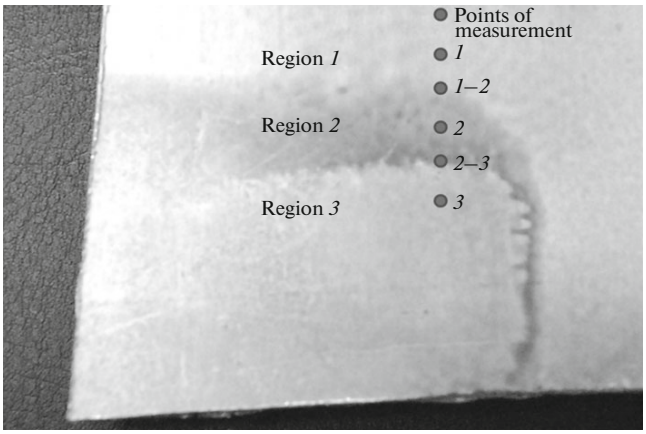

Fig. 4. Reference area at the periphery of a sample after laser irradiation. Region *1* was unaffected; region *2* was revealed after the deposition of contrasting material; region *3* was subjected to irradiation. Points *1–2* and *2–3* mark the boundaries between regions *1*, *2*, and *3*.

reflected from the oxide and metal surfaces. This allowed us to measure the thickness of the Al_2O_3 layers (~7 μm) on the initial surfaces. To study their relief, each surface was decorated by sputtering a thin film of contrasting material (titanium).

Processing of the obtained data revealed three distinct regions on each surface (see Fig. 4): nonirradiated region *1*, region *3* subjected to intense irradiation, and boundary area *2* of the irradiated region.

The external appearance and a plotted three-dimensional image of the relief of a typical part of these regions are shown in Fig. 5. Surface roughness on the order of 2–3 μm orthogonal to the mechanical processing scratches was detected on each initial surface. Each surface appeared to be relatively smooth and free of notable local distortions along these lines (Figs. 5a, 5b).

The surface properties changed fundamentally upon moving to the region subjected to laser irradiation: each surface becames rough and spotted with craters with depths of several micrometers. Two- and three-dimensional and profile images (obtained using a Zygo optical interferometer) of characteristic regions of the disks made from D16 alloy and traces of laser irradiation are shown in Fig. 5.

X-ray diffraction studies showed that the elemental composition of the coating was virtually unchanged after laser irradiation. Its primary components were aluminum and oxygen with admixed sulfur (the same as in the initial composition of the surface layer). The phase composition of surfaces modified by laser irradiation was, however, altered drastically.

It was found that the primary reflections off a sheet's initial surface at the analyzed depth of ~2–3 μm were from the aluminum phase. Weak reflections from the passivated films of aluminum oxide were also present. In the regions subjected to laser irradiation, the surface layer was a polycrystalline aggregate of different nonequilibrium aluminum oxide phases (monoclinic, hexagonal, and rhombohedral Al_2O_3) and compounds of aluminum with manganese (Al_6Mn and $Al_{19}Mn_4$) and magnesium (Al_3Mg_2, $Al_{12}Mg_{17}$, and AlMg).

The measurements performed using a Zygo NewView 5000 profilometer showed that the initial surfaces had aluminum oxide layers ~7 μm thick. In [12], we found that absorption coefficient β of Al_2O_3 at 10.6 μm must be ~$(2–3) \times 10^4$ cm^{-1} by approximating the data from [13], in which the coefficient of absorption for sapphire in the visible and IR regions of the spectrum (up to 7 μm) was given. In accordance with Bouguer's law, radiation was attenuated by a factor of e in an Al_2O_3 layer ~0.5 μm thick. Using reference data on the thermophysical properties of Al_2O_3 [14, 15] (specific heat capacity at $T = 1300$ K, 1.3 J/(g K)$^{-1}$; $T_m = 2015$ K; heat of melting, 109 J g^{-1}; boiling temperature, ~3500 K; heat of evaporation, 6.61 kcal mol^{-1}) and ignoring heat conductivity and heat losses for

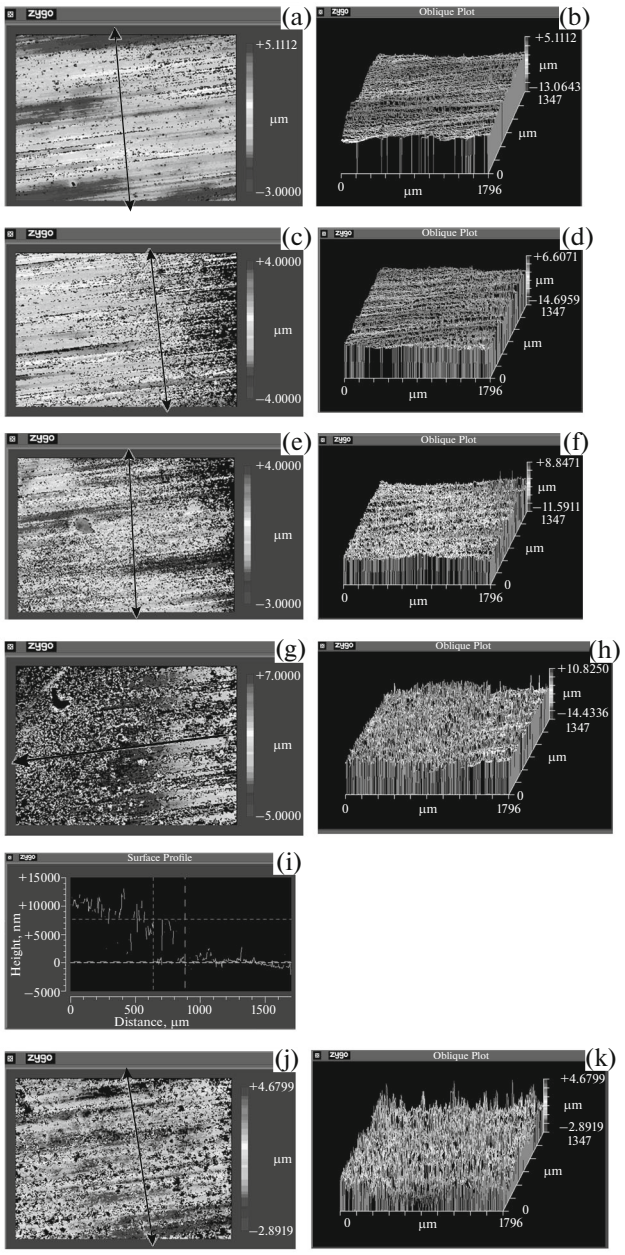

Fig. 5. Two- and three-dimensional and profile images (obtained using a Zygo optical interferometer) of characteristic regions of disks made from D16 alloy with marks left by laser irradiation: (a, b) area *1* in region *1* (Fig. 4), R_a = 817 μm; (c, d) area *1–2* at the boundary between regions *1* and *2*, R_a = 770 μm; (e, f) area *2* in region *2*, R_a = 796 μm; (g–i) area *2–3* at the boundary between regions *2* and *3*, R_a = 1806 μm; and (j, k) area *3* in region *3*, R_a = 788 μm. Frame size, 1796 × 1347 μm.

reradiation on the one hand, and the contribution to heat balance from the optical air breakdown plasma, where most of the energy of the laser pulse tail is released on the other, we estimated that an energy release of ~1 J cm^{-2} in a thin Al_2O_3 surface layer is enough to heat this layer to the temperature of evaporation. The estimated value corresponds to the energy density at the peak of a laser pulse that reaches the sample surface. This correlates with the results obtained via scanning electron microscopy.

It is clear from Fig. 3 that a foamy surface layer formed, while the optical profilometry data (Fig. 5) indicate that the aluminum oxide layer, which had an initial thickness of ~7 μm, grew somewhat thinner and was modified. The microphotographs show that the scratches on the duralumin surface remained, although a number of new defects formed in the oxide layer above these scratches; i.e., irradiation left almost no marks on the surface of metal itself.

At the same time, it is seen clearly in Fig. 5 that region *2* is ~10 μm higher than region *3*. This difference is greater than the initial oxide layer thickness. This apparent contradiction is easily resolved: owing to dynamic gas processes in a plasma plume, a considerable part of the evaporated Al_2O_3 condensed at the periphery of the irradiated region and formed region *2*. Since the cooling of the melt and the condensation of evaporated material take several microseconds, the material in a surface's aluminum oxide layer undergoes numerous structural changes that result in the formation of a number of transition modifications in the sequence of phase transformations γ-$Al_2O_3 \rightarrow$ α-Al_2O_3 [1]. Our results correlate with the ones reported in [16], where the interaction between a CO_2 laser pulse and aerosol aluminum oxide particles with diameters of 0.7 μm was studied. At a pulse duration of 3 μs, a radiation power density of ~1–5 MW cm^{-2} is needed to evaporate them.

CONCLUSIONS

The interaction between CO_2 laser pulses and an aluminum oxide layer must be considered in studies focused on developing the technology for laser cutting of the surfaces of items made from aluminum and its alloys. In addition, our data can be used to develop a technique for modifying surfaces of passivated aluminum alloys in order to form ornamental or labeling patterns or inscriptions.

ACKNOWLEDGMENTS

This work was performed as part of State Task no. 26.1326.2014/K ("Developing a Theoretical and Methodological Background for the Sustainable Growth of and Innovative Economy and Stimulating the Demand for Innovation in Russia") of the RF Ministry of Education and Science.

REFERENCES

1. Krushinskaya, L.A. and Stel'makh, Ya.A., *Vopr. At. Nauki Tekh., Ser.: Vak., Chist. Mater., Sverkhprovodn.*, 2011, no. 6, p. 92.

2. *GOST* (State Standard) *21631-76: Sheets of Aluminum and Aluminum Alloys. Specifications*, 1976.
3. Konov, V.I., Optical breakdown of gases near the surface of solids, *Extended Abstract of Doctoral (Phys.–Math.) Dissertation*, Moscow, 1982.
4. Alikhanov, A.N., Bakeev, A.A., Vas'kovskii, Yu.M., et al., in *Lazernye i opticheskie sistemy* (Laser and Optical Systems), Moscow: GNTs NPO Astrofizika, 1994, p. 136.
5. Vas'kovsky, Yu.M., Gordeeva, I.A., Korenev, A.S., et al., *Proc. SPIE*, 1990, vol. 1440, p. 229.
6. Babaeva, N.A., Vas'kovsky, Yu.M., Zhavoronkov, M.I., et al., *Proc. SPIE*, 1990, vol. 1440, p. 260.
7. Barchukov, A.I., Bunkin, F.V., Konov, V.I., and Lyubin, A.A., *J. Exp. Theor. Phys.*, 1974, vol. 39, no. 3, p. 469.
8. Levinzon, D.I., Rovinskii, R.E., Rogalin, V.E., et al., *Izv. Akad. Nauk SSSR, Ser. Fiz.*, 1979, vol. 43, no. 9, p. 2001.
9. Apollonov, V.V., Vas'kovskii, Yu.M., Zhavoronkov, M.I., et al., *Quantum Electron.*, 1985, vol. 15, no. 1, p. 1.
10. Rogalin, V.E., *Izv. Vyssh. Uchebn. Zaved., Mater. Elektron. Tekh.*, 2013, no. 2, p. 11.
11. Rogalin, V.E., *Materialovedenie*, 2013, no. 9, p. 34.
12. Rogalin, V.E., Kaplunov, I.A., Tsenina, I.S., and Andreeva, M.C., in *Materialy XXI vseros. konf. "Optika i spektroskopiya kondensirovannykh sred"* (Proc. XXI All-Russian Conf. "Optics and Spectroscopy of Condensed Media"), Krasnodar, 2015, p. 55.
13. Lingart, Yu.K., Petrov, V.A., and Tikhonova, N.A., *Teplofiz. Vys. Temp.*, 1982, vol. 20, no. 5, p. 872.
14. Blistanov, A.A., Bondarenko, V.S., Perelomova, N.V., et al., *Akusticheskie kristally: spravochnik* (Acoustic Crystals: Handbook), Shaskol'skaya, M.P., Ed., Moscow: Nauka, 1982.
15. *Tablitsy fizicheskikh velichin: spravochnik* (Tables of Physical Quantities: Handbook), Kikoin, I.K., Ed., Moscow: Atomizdat, 1976.
16. Bakulin, I.A., Kazakevich, V.S., and Pichugin, S.Yu., *Tech. Phys.*, 2006, vol. 51, no. 11, p. 1490.

Translated by D. Safin